

RESEARCH PAPER

Improve the Medical Properties of Nanocomposite Metal Oxide by Increase the Activity

Usama S. Altimari¹, Ola Kamal A. Alkadir¹ Firas H. Abdulrazzak² Ayad F. Alkaim^{3*}

¹ Department of Medical Laboratory Techniques, Al-Nisour University College, Iraq

² College of Science, Forensic Evidence Department, Al-Karkh University of Science, Iraq

³ College of science for women, University of Babylon, Iraq

ARTICLE INFO

Article History:

Received 08 March 2021

Accepted 13 June 2021

Published 01 July 2021

Keywords:

Nanocomposites metal Oxide

Photocatalytic activity

Sol-Gel

Staphylococcus aureus

ABSTRACT

In this work, Enhancement activity of nanocomposite metal Oxide by laser for medical application, nanocomposite metal Oxide we prepared by using a simple Sol-Gel method that used to synthesize and measure (, ZnO/and Cu: ZnO/). X-ray diffraction (XRD) was used to describe the crystalline structures, Cu₂O spikes were observed (26.393 °), and the amplitude of these peaks became high with a copper concentration that explained a higher Cu₂O mass fraction was provide from the copper load. The pictures from the FTSEM showed that most particles are spherical. The effect of heat treatment and laser on the particle size was substantial as well. The chemical bonds and the functional groups of TiO₂ NPs were analyzed using Fourier Transform Infrared Spectroscopy (FTIR) within a 400-4000 cm⁻¹ wavenumber range. The solid and broad O-H stretching peaks, C-H bending, N-H bending, and C-Cl stretching chemical bonds were obtained. The photocatalytic activity of (, ZnO/and Cu: ZnO/) were then evaluated under laser rays. ZnO/TiO₂ were calcination at 500 °C showed the highest photoactivity compared to that calcination at 400, 600, and 700°C That has the top activity than Cu: ZnO/TiO₂ and titanium oxide consequently The antibacterial activity of the prepared specimens was indicated by the Kirby-Bauer disc method that Enhancement photocatalytic activity by laser. ZnO/TiO₂ NPs showed a very efficient antibacterial action against Staphylococcus aureus strains extraordinary antibacterial efficacy against S. aureus bacterium strains

How to cite this article

Altimari U. S, Alkadir K. A. O. Abdulrazzak F. H, Alkaim A. F. Improve the Medical Properties of Nanocomposite Metal Oxide by Increase the Activity J Nanostruct, 2021; 11(3):568-576. DOI: 110.22052/JNS.2021.03.014

INTRODUCTION

Nanotechnology has been thriving to develop different main activities in recent years because the materials have unique properties, including nanomaterials. [1]. Nanostructured materials receive a great deal of attention, especially in biological and pharmaceutical applications, due to their potential for specific procedures and selectivity [2]. Photocatalysis is a flexible and highly versatile process that may be used for many water and air disinfection applications. Though, self-disinfection surfaces have been created and verified for usage in the form of goods being sold. [3] Chromium, iron, nickel, zinc, and copper are transition metals. [4,5] and Cu, copper with 0.52 V (Cu²⁺) and 0.16 V (Cu²⁺) (Cu¹⁺). For several photocatalysts, redox potential was found to be an appropriate match [4]. (Cu²⁺) (0.73 Å), (Cu²⁺) (0.83 Å) and (Ti⁴⁺) (0.64 Å) have exact ionic density sizes (Cu²⁺) will be able to break through or eliminate the surrounding oxygen vacancy TiO₂ and ZnO deep acceptor matrices (Zn²⁺) or (Cu¹⁺) positions [6]. Nanotechnology has given rise to a new generation of biocidal agents, and they can even be tailor-made to produce microscopic particles of any shape and size. The results of

various studies demonstrate that nanoparticulate formulations are powerful bactericidal agents. Suspensions that are lit up TiO₂ support the research and development of photocatalytic techniques to eradicate Escherichia coli, the microorganism responsible for enteritis, hemorrhagic colitis, and diarrhoea. TiO₂ in aqueous media [7]. The gram+ cocci-shaped staphylococcus aureus bacterium may be discovered on human skin, the nose, or the respiratory tract [8-10]. The two primary goals of this investigation are [1] to assess the use of visible laser diodes as a light source for photocatalytic degradation enhanced metal oxide photocatalytic activity and [2] to evaluate the catalytic capabilities of -> The overall goals of this study are to examine the use laser diodes for photocatalytic degradation that are visible to the naked eye enhanced metal oxide photocatalytic activity and to determine the catalytic capabilities of -> These are the two primary objectives of this study: [1] to examine the feasibility in the photocatalytic breakdown of enhanced metal oxide photocatalytic activity and [2] to determine the catalytic capabilities of -> TiO₂, ZnO/ TiO₂ and Cu: ZnO/ TiO₂ NPs under laser light irradiation.

* Corresponding Author Email: alkaimayad@gmail.com

MATERIALS AND METHODS

The applied precursors can be listed as: The titanium trichloride (TiCl₃ 15% solution in HCl, Sigma–Aldrich, Germany), ammonium hydroxide (NH₄OH 30-33% NH₃), zinc chloride (ZnCl₂ 99%), sodium hydroxide (NaOH from Sigma–Aldrich, Germany). The cupric nitrate trihydrate was applied for doped samples.

Preparation (TiO₂, ZnO, ZnO/ TiO₂, Cu: ZnO/ TiO₂)

TiO₂ NPs have been produced using a sol-gel technique at PH=10. The reaction was performed at 50 °C under vigorous stirring at 700 rpm. Firstly, the “sol” was prepared by mixing TiCl₃ with NH₄OH as a procedure. Secondly, the “sol” grows into a gel phase system containing both a liquid and a solid phase. Thirdly, a drying process was used to remove the remaining liquid phase. The situation is often followed by substantial shrinkage. To finish, it’s common to need heat treatment, or calcination procedure, to acquire the finished product. The decline that often follows this scenario is typically significant. To finish, it’s common to need heat treatment, or calcination procedure, to acquire the finished product.

In contrast, the situation is often followed by substantial shrinkage. To finish, it’s common to need heat treatment, or calcination procedure, to acquire the finished product. Which is typically accompanied by a significant amount of shrinkage. Finally, a thermal treatment, or calcination process, is often necessary to obtain the final nanopowders. ZnO was prepared by the sol-gel method, where ZnCl₂ and NaOH was analyzed in the presence of a controlled amount of ethanol as a 1: 2 solvent. We put the solutions on the ultrasound machine for five minutes, then put them on the stirring device at a temperature of 60 degrees Celsius for an hour; after the solutions are dried to get rid of the liquid materials, here the heat treatment or calcination is done to obtain the ZnO nanoparticles, and to preparation TiO₂/ZnO After and ZnO reach the gel phase, equal amounts of titanium oxide and zinc oxide gel are taken and mixed and placed in one baker and on Stirrer at 60

° C for one hour, then washed, dried and calcined at different temperatures(400, 500,600, and 700 °C), and to preparation Cu: ZnO/TiO₂. After the preparation of ZnO/TiO₂ nanoparticles and reach the pre-washing stage, dissolve the aqueous copper nitrate according to the molar equation and add it gradually to the two compounds, taking into account the constant stirring for 30 minutes, then wash, dry and calcination at a temperature of 500 to obtain a tinged nanomaterial.

RESULTS AND DISCUSSION

Properties of the structural

X-Ray Diffraction (XRD) of TiO₂ measurement

The XRD of the TiO₂ NPS at 400, 500,600, and 700 °C calcination identify the peaks of anatase (A) and rutile (R) phases. (400, 500, and 600 °C) show the anatase only 700 °C present anatase-rutile phase at (700 °C). However, the pattern shows that and at (400 °C) has three broad peaks at 2θ equal 27.757, 40.303, and 50.451, with (101), (004), and (200) diffraction planes, respectively. The sample calcination at (500 °C) has three broad peaks 2θ angle at 27.900, 40.451, and 50.602 with (101), (004), and (200) in the plane of diffraction, each time. The NPS of calcination at all the temperatures was determined as indicated in the Scheme. 1 that prove we get the perfect structure of TiO₂ NPS. However, the slight change may be drawn to the interaction processor to combine two phases in the same part-scale (Fig. 1).

X-Ray Diffraction (XRD) of ZnO/ TiO₂ measurement

Fig. 2 shows the XRD result of NPs prepare at different treatments, which reveals ZnO and TiO₂ in all the samples. The ZnO may be found in the samples as zincite-phase TiO₂ Titania is in the anatase phase with no polymorphs present. Polymorphic titanium dioxide was discovered by examination of the sample, but no additional polymorphs were found. It is clear that the TiZ400 pattern that (101) happened to be the most potent reflection of both ZnO and TiO₂. A gradual reduction from TiZ400 up to TiZ700 for mole fraction is observed in Fig. 2. According to Fig. 2, heat treatment from 400 up to

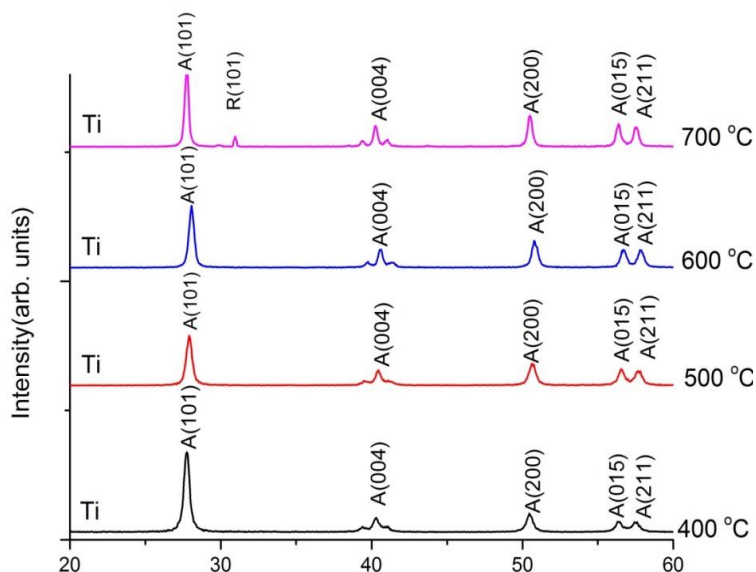


Fig. 1. XRD patterns of The calcination produced different NPS compositions at different temperatures. (400, 500,600, and 700 °C) (A anatase and R rutile).

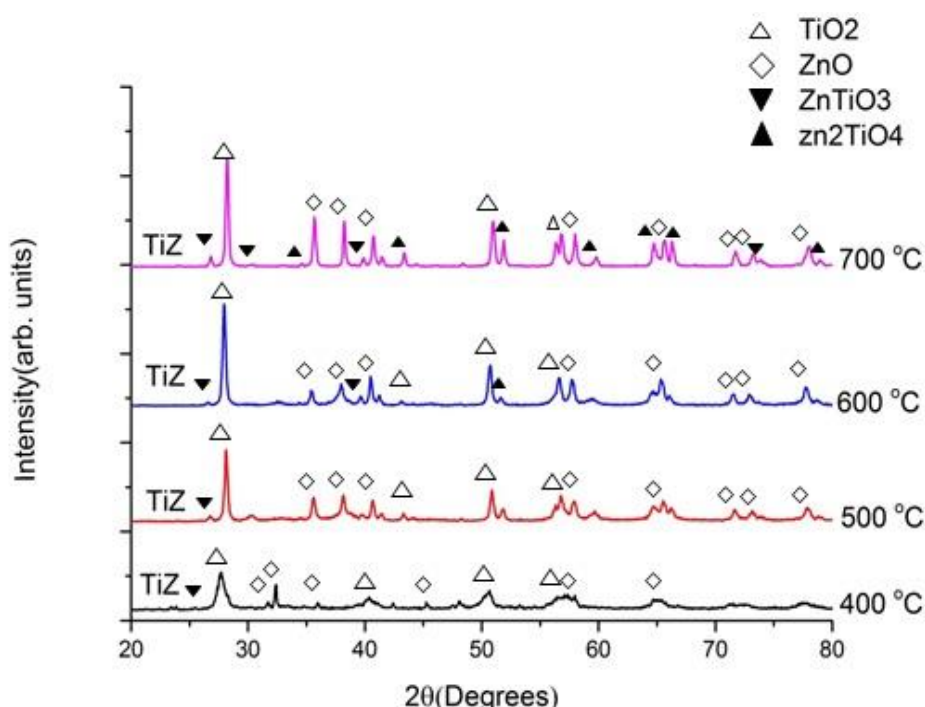


Fig. 2. XRD of sample and calcination ZnO / TiO₂ composites at 400, 500, 600, and 700 °C (TiZ400, TiZ500, TiZ600, and TiZ700).

700 °C decreases the intensity of the (101) plane of Anatase, while (002) ZnO plane rises slowly. It shows that atoms of Zn on the (002) plane were ideally replaced by atoms of Ti and the formation of a ZnO/TiO₂ the solid solution has been continued gradually by the increase of calcination temperature. By increasing temperature from 400 up to 700 °C, the intensity of ZnTiO₃ is getting a gradual decrease.

X-Ray Diffraction (XRD) of Cu: ZnO/TiO₂ measurement

XRD showed the structures of Cu: ZnO/ TiO₂ indifferent TiO₂ and ZnO level and temp. Fig. 3 shows the XRD of the samples consist of 1–4 wt% copper, temp at 500 °C (Fig. 3). Zinc Oxide Quality JCPDS (reference code 98-002-9272), crystal phases of TiO₂ including anatase (00-021-1272), Rutile (01-075-

1750) and Brookite (00-029- 1360), Cu₂O (00-05-0667) and CuO (00-48-1548) Are used to determining trends. Cu: ZnO/ TiO₂ with copper loading of 1 wt% that temp at 500 °C. It crystallized in a matrix as Fig. 3, among TiO₂ crystal structures, Anatase diffraction peaks showed the Strongest intensities at 500 ° C after calcination, Indicating their main phases inside the photocatalyst at this point. In the meantime, signs of rutile are also observed at 500 ° C in Cu: ZnO / TiO₂ calcination. Using the sol-gel method, anatase structure is generally generated in TiO₂ synthesis. However, rutile is stable, whereas brookite and Anatase are metastable. Besides TiO₂ crystals, ZnO with peak intensities of intense diffraction are found in these photocatalysts. However, several ZnO In this study peaks based not identifiable on standard

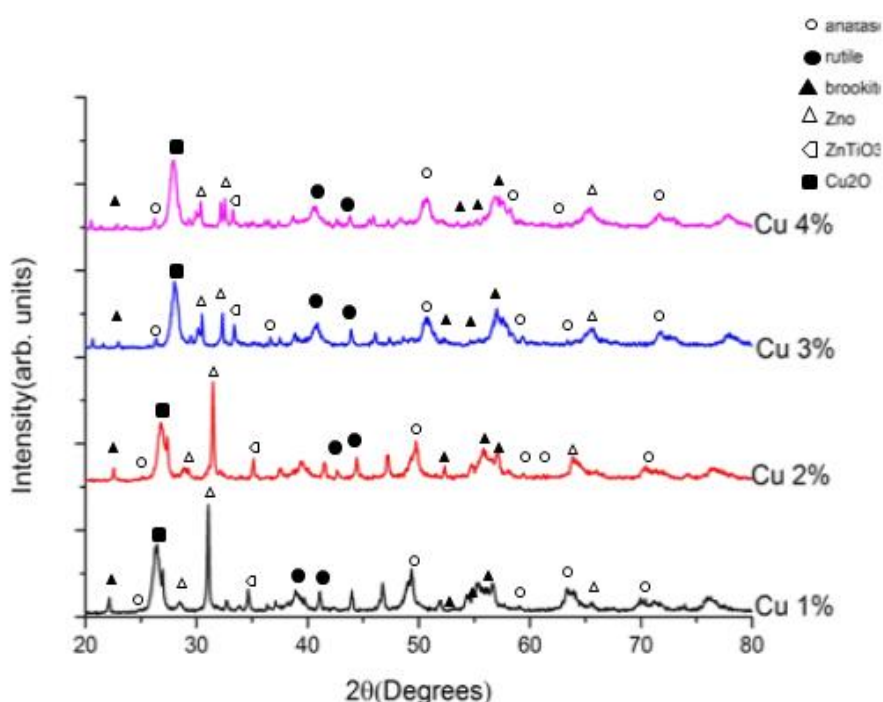


Fig. 3. XRD of Cu: ZnO/ TiO₂ calcination at a 500°C when Cu (1 %, 2%,3%, and 4%)

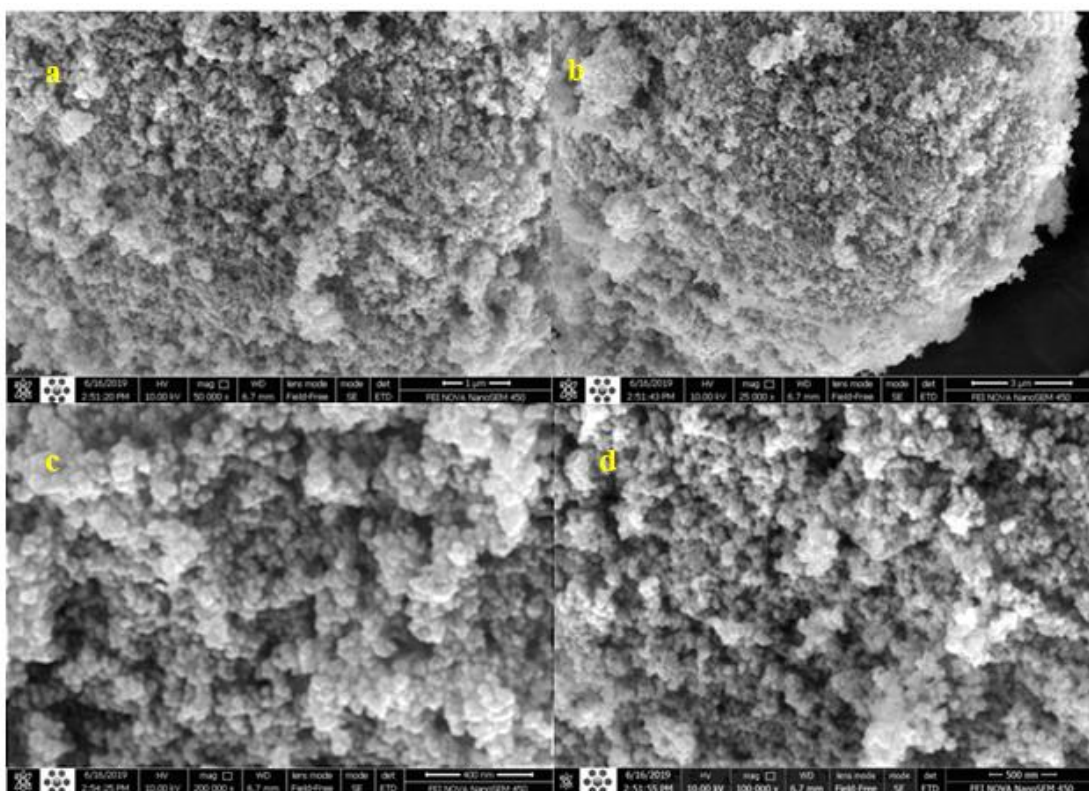


Fig. 4. FESEM pictures depict the shape of the surface TiO_2 NPS For magnifications 10.00KX, at a calcination temperature of 500 °C, (a-1 μm), (b-3 μm), (c-400 μm), and (d-500 μm)

peaks. The findings proved that photo-depositional modification was successful. ZnO's basic crystal structure and its transformation into ZnTiO_3 or ZnTiO_4 . In this instance, it may be owing to the even dispersion of copper nanoparticles. ZnO surface. On the other hand, the presence of a high amount

of zincite in the calcination of samples at 500 ° C indicated that the transformation mentioned above for photocatalysis at that temperature was not fully achieved. According to the Fig. 3, Signals of Cu_2O (26.393 °) was detected, and the amplitude of these peaks increased with the concentration of copper,

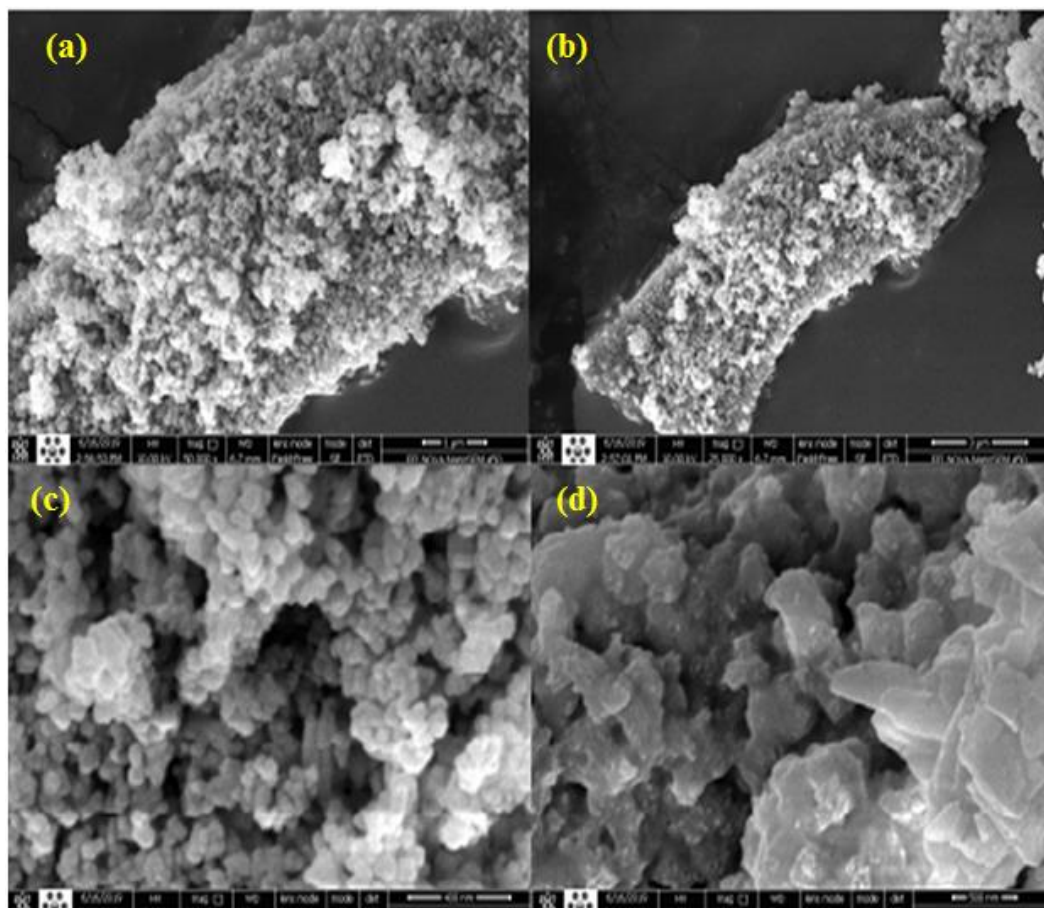


Fig. 5. FESEM imaging is used to reveal the surface topography. ZnO/TiO_2 NPS at magnification (a-1 μm), (b-3 μm), (c-400 μm), and (d-500 μm) at a calcination temperature of 500 °C

which explained the higher mass proportion of Cu_2O with copper heating. However, Cu_2O the o diffraction pattern is not observed as CuO Or due to the XRD detection cap, the limited size of Cu components. Another potential explanation may be a strong CuO dispersion inside the TiO_2 frameworks.

Electron Scanning Microscopy for Field Emission (FESEM) of TiO_2 measurements

Surface morphology and growth of the NPS is Reviewed by the Field Emission Scanning Electron Microscopy (FESEM)., Fig. 4 shows the surface morphology of the TiO_2 NPS samples calcination at 500°C at different magnification. The average particle size is calculated as shown in Table 1. The results show the larger particle size with a high uniform morphology for calcination of the samples at 500°C .

Field Emission Scanning Electron Microscopy of ZnO/TiO_2 Measurements

Fig. 5 shows the top surface of the ZnO/TiO_2 nanocomposites, which demonstrates the relationships to crystallography among the TiO_2 nanoparticles and ZnO nanorods template. For the nanocomposites, TiO_2 nanocomposites prepared by the thermal method at 500°C , The average particle size of the composites is about 500 nm . The FESEM images show the uniform sizes of the nanocomposite particles prepared at 500°C temperatures. Also, FESEM images provided additional information, including the structures and surface morphologies of the as-prepared nanomaterials. As shown in Fig. 5, by taking the best samples at temperatures on calcination (500°C) with magnification (a- $1\mu\text{m}$), (b- $3\mu\text{m}$), (c- $400\mu\text{m}$), and (d- $500\mu\text{m}$) As for the as-prepared ZnO/TiO_2 nanocomposite (TiZ500, a- $1\mu\text{m}$), it can be seen that TiO_2 nanoparticles are well

distributed over ZnO nanorods (Fig. 5-a), which also indicated that the original Building and shape of the TiO_2 nanoparticles and ZnO nanorods are well preserved during the preparation of the ZnO/TiO_2 nanocomposites.

Field Emission Scanning Electron Microscopy of $\text{Cu}:\text{ZnO}/\text{TiO}_2$ Measurements

According to the findings presented in Fig. 6, the $\text{Cu}:\text{ZnO}/\text{TiO}_2$ photocatalyst morphology was affected by copper doping as demonstrated in Fig. 6 using FESEM. the impact of calcination temperature is shown in (1wt percent) whereas the influence of calcium hydroxide solution concentration is shown in -> The effect of calcium hydroxide solution concentration is shown in (1wt percent) as compared to (Fig.6-b). The XRD examination shows that the photocatalyst with 1.0 wt, as indicated, was produced at 500°C and is primarily composed of amorphous crystals. This finding is further backed up by the FESEM picture shown below (Fig. 6-a). As shown, the catalyst's surface is smooth and non-abrasive. The XRD results indicate that either the rutile nucleation sites or the adsorbed photocatalyst surface may be explained by the presence of an increased dopant concentration. The FESEM pictures showed crystalline lattice alterations in the photocatalyst array caused by the increase in dopant data (Fig. 6-b). The following image (Fig 6-c) demonstrates that when the magnification increased to $500\mu\text{m}$, the crystallinity may have grown and become more pronounced. Cu doping also led to an improvement in crystallinity as a side effect of dopant concentration. This conclusion is consistent with the results of the XRD study. $\text{Cu-ZnO}/\text{TiO}_2$.

Structures of the TiO_2 UV-vis spectroscopy

Using the U.V.-vis spectroscopy for determining an optical property of TiO_2 . Fig. 7 shows the absorption

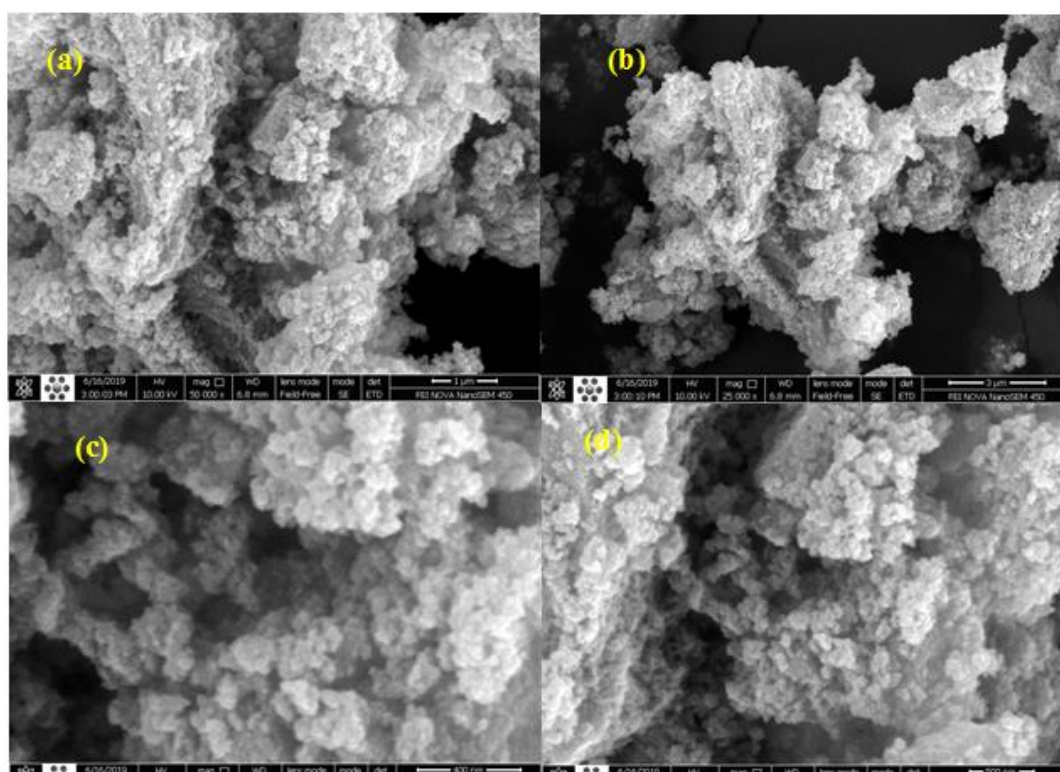


Fig. 6. The surface morphology is defined using FESEM images. of $\text{Cu}:\text{ZnO}/\text{TiO}_2$ NPs with calcination temp 500°C and Cu 1% of magnifications 10.00KX at magnification (a- $1\mu\text{m}$), (b- $3\mu\text{m}$), (c- $400\mu\text{m}$), and (d- $500\mu\text{m}$)

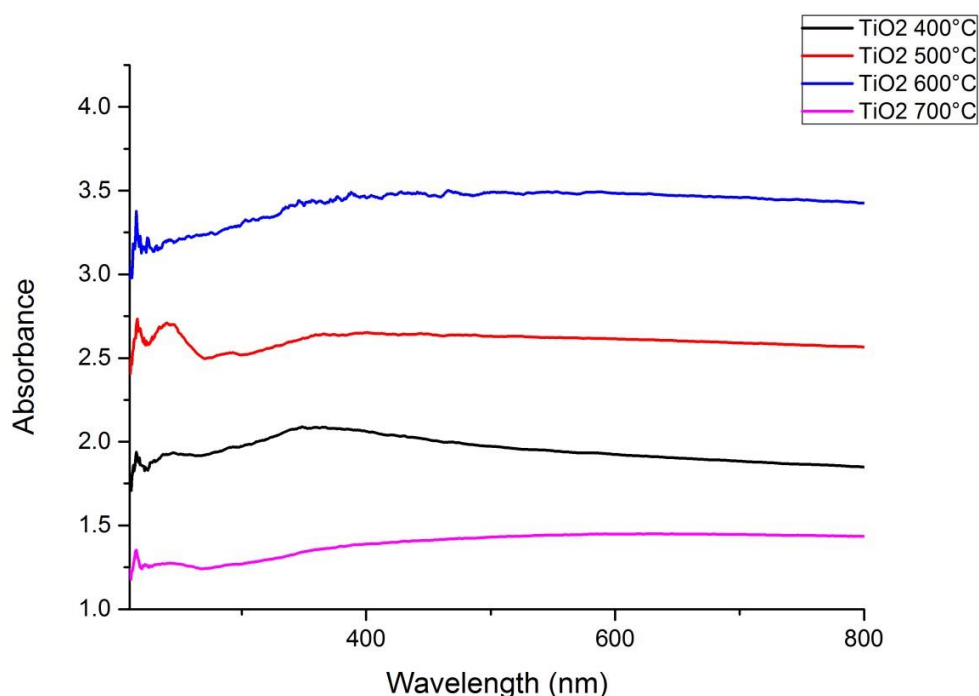


Fig. 7. U.V.-vis absorption spectra of TiO₂ nanoparticles many (400-700) °C temp.

Table 1. Average particle size of (TiO₂), (ZnO/ TiO₂), and (Cu: ZnO/ TiO₂) NCM synthesized at temperatures on calcination (500 °C).

Nanocomposite	Minimum P.S (nm)	Maximum P.S (nm)	Average particle size (nm)
TiO ₂	36.30	62.11	46.53
ZnO/ TiO ₂	35.18	55.62	45.36
Cu:ZnO/ TiO ₂	62.29	337.2	190.55

Table 2. As-synthesized optical band gap TiO₂ samples at many temps

Sample	Band-gap Eg (eV)
TiO ₂ calcination at 400 °C	3.02
TiO ₂ calcination at 500 °C	2.95
TiO ₂ calcination at 600 °C	2.75
TiO ₂ calcination at 700 °C	2.55

of the TiO₂ nanoparticles at any temp. The bandgap energy is measured depending on the equation [1]:

$$E_g = 123.8 / \lambda \tag{1}$$

E_g is the Band gap and λ is the wavelength.

λ is the Bandgap was measured optically using the above method at several different temperatures as Table (2).

Fig. 7 shows TiO₂ nanoparticle at temp (400) °C at (410) nanometer attributed to the band gap is 3.02 eV with delicate anatase phase and show highly crystalline nanomaterial. The TiO₂ samples calcination at 500 °C, 600 °C and 700 °C show absorption at the wavelength (420) and (450) nanometer. At high temp, the TiO₂ is change the absorption from UV to visible light.

UV-Vis spectroscopy of ZnO/ TiO₂ structures

UV-Vis diffuse reflectance spectra analysis the optical absorption properties play an essential role in evaluating the photoabsorption ability of photocatalyst. Fig. 8 shows the U.V.-Vis diffuse reflectance spectra of as-prepared samples ZnO/ TiO₂ at (400-700) °C temperatures. U.V. absorption was dominant across the span of nearly the whole U.V. spectrum. (λ=233 nm) at 700 °C, and the weak absorption happened in the visible region for ZnO/TiO₂ at 400 °C. Furthermore, the absorption edge spread into the visible light range when temperatures increased. Furthermore, when temperatures increase, the absorption edge spreads into the visible light range. ZnO/TiO₂ at 500°C and 600 °C. Notably, the absorbance intensity of ZnO/

TiO₂ at 600 °C in the visible light region is more vital than that of ZnO/TiO₂ 500 °C, which illustrated those doping zinc elements facilitated the extending of optical absorption toward the visible light region.

UV-vis spectroscopy of Cu: ZnO/ TiO₂ nanoparticles structures

The absorption spectra of undoped and doped samples were measured in the UV-visible range. Cu: ZnO/ TiO₂ nanoparticles are shown in Fig. 9. It can be seen in Fig. 9 that there is a strong excitonic absorption peak in all samples. This peak is attributed to the large binding energy of excitons and the good optical quality of nanoparticles. With the increasing Cu content, the redshift is slight in band edge absorption peak. The calculated bandgap

of the Cu:ZnO nanoparticle are 3.297, 3.28, 3.263, and 3.53, TiO₂ nanoparticle are 3.02, 2.95, 2.75, and 2.55 for 1%, 2%, 3% and 4% doping respectively. The bandgap decrease with Cu doping concurs with previous studies on Cu doping. ZnO/ TiO₂. Two leading causes may contribute to variations in bandgap energies, namely quantum size effect and electronic structure modifications. Because of the Bohr radius of ZnO and TiO₂ is in the range 0.9–2.4 nm, the decrease of the band gap in Fig. 9 is not likely due to samples of as-synthesized material exhibit diameters greater than 60 nm. It is reasonable to expect the slight band gap (E_g), decrease with Raising in concentrations of Cu as possibly due to doping induced band edge Bowing.

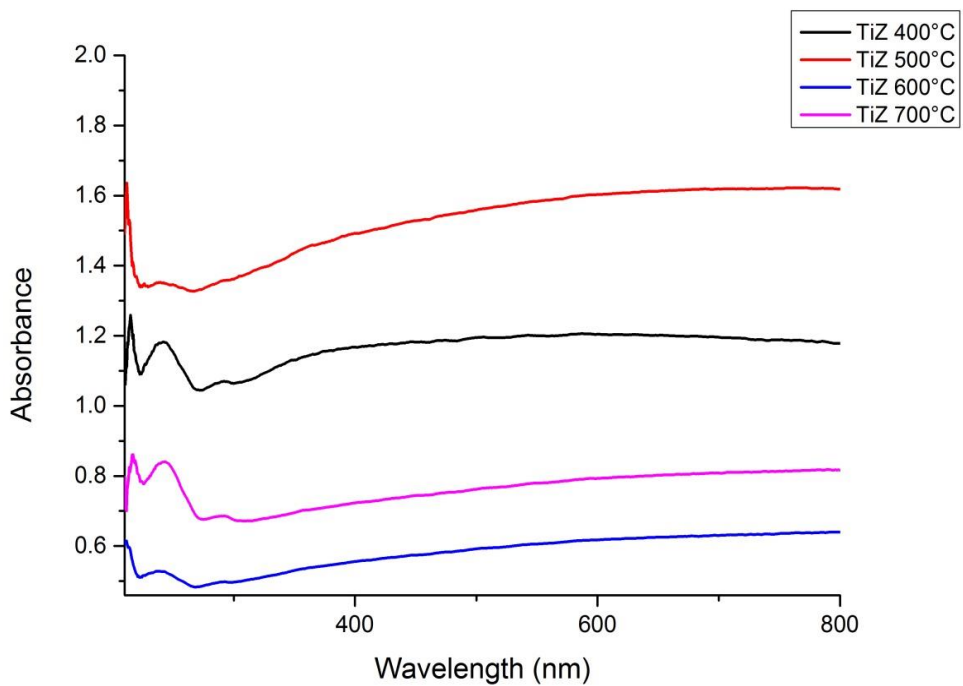


Fig. 8. Absorption spectra for U.V.-vis. ZnO/ TiO₂ nanoparticles temp (400-700) °C.

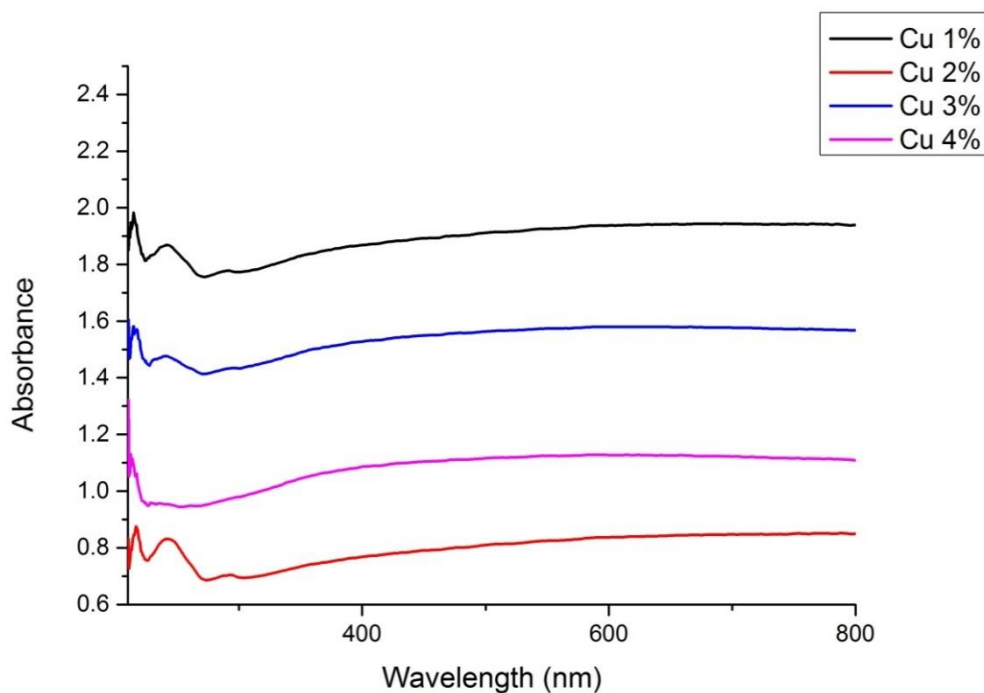


Fig. 9. U.V.-vis absorption spectra of Cu: ZnO/ TiO₂ nanoparticles calcination at 500 °C temperatures and with doping for Cu 1%,2% 3% and 4%.

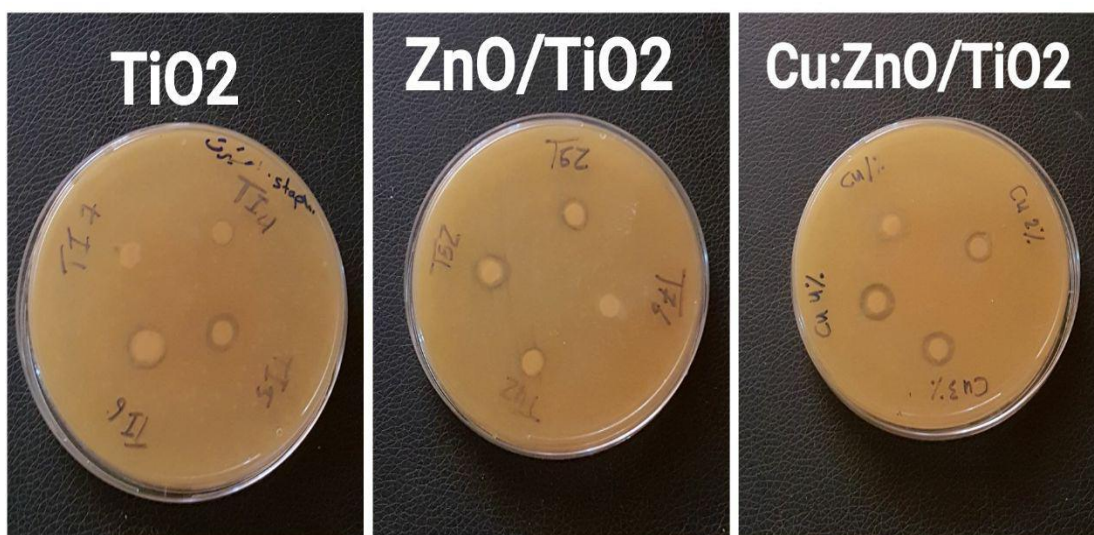


Fig. 10. shows images of the antibacterial activity of , ZnO/ TiO₂, Cu: ZnO/ TiO₂ against Staphylococcus aureus

Table 3. The zone of suppression of bacterial growth TiO₂, ZnO/And Cu: ZnO/N.P.s without laser at 400-700°C against Staphylococcus aureus.

Nanocomposite	Inhibition zone diameter (mm), without laser			
	Calcination temp (400 °C)	Calcination temp (500 °C)	Calcination Temp (600 °C)	Calcination Temp (700 °C)
TiO ₂	2	3	2	-
ZnO ₂ / TiO ₂	2	4	2	-

Table 4. Zone of bacterial growth inhibition of Cu: ZnO/ TiO₂ NPS without laser against Staphylococcus aureus with temperatures on calcination (500, °C) and at 1%, 2%, 3%, and 4%.

Nanocomposite	Calcination temperature	1 %	2%	3%	4%
Cu:ZnO/ TiO ₂	500 °C	11	12	10	14

Antibacterial activity of TiO₂, ZnO/TiO₂, Cu: ZnO/TiO₂ NPs Measurements

The pictures of antibacterial activity shown in Fig. 10 were seen using the zone of inhibition analysis, with or without laser treatment. TiO₂, ZnO₂/TiO₂, Cu: ZnO/TiO₂ against Staphylococcus aureus. Table (3) for the four specimens in the test, this image illustrates the antibacterial activity findings. (400-700 °C). The inhibition zone diameter was measured in mm, and Table (4) show the results of the antibacterial activity test for Cu: ZnO/ TiO₂ specimen with temperatures on calcination (500 °C) at 1%, 2%, 3%, and 4%. The inhibition zone diameter was measured in mm.

When the temp of TiO₂ N.P.s become more leads to the decreasing of the inhibition. The cause of increasing inhibition was attributed to increasing the surface area of the reaction as the particle size of TiO₂ NPs decreased.

Disc diffusion to measure the antibacterial activity of nanoparticles, it was completed. ZnO/ TiO₂. Inhibition zone diameter indicated that ZnO/

TiO₂ in 500 °C had a more significant antimicrobial effect against bacteria compared to the combination of individual nanoparticles with 400 °C, 600 °C, and 700 °C. Based on the results, S. aureus bacteria were more sensitive to the antimicrobial agents in ZnO/ TiO₂ more than. The primary purpose of using ZnO as a nanocomposite with TiO₂ is to control their release of and increase the antimicrobial activity. The permeability of both the cell wall and the cell membrane is disrupted by nanoparticles, thereby interfering with DNA replication and protein synthesis.

Photocatalytic activity and antibacterial experiments were executed Cu doped ZnO/ TiO₂ at 1%, 2%, 3%, and 4% with a temperature of 500 °C. In addition, this data was compared to new results. TiO₂ and ZnO/ TiO₂. The samples were evaluated with bacterial strains S. aureus. The bacterial Inhibition zone diameter significantly is increasing at 1%, 2%, and 4%. The bacterial reduction was achieved in the presence of Cu doped samples in 3%.

the inactivation observed is a synergetic effect of TiO_2 . As well as Cu ions in the presence of visible light were introduced and led to enhanced absorption efficiency, which made bacterial inactivation faster, as shown in comparison to control samples.

CONCLUSION

The crystalline lattice strengthened with an increase in the dopant matrix content and temp. Both TiO_2 Anatase and ZnO Wurtzite phases were obtained without impurity compounds, as shown in the XRD patterns. After calcination, the anatase peaks (004) and (101) in the nanocomposite respectively appeared at 400, 500, and 600 °C, while the Rutile peaks appeared in the 700 °C. FTSEM results showed that spherical TiO_2 rod-like ZnO particles were obtained. TEM results confirmed that the spherical TiO_2 particles were embedded in the lattice and attached to the ZnO rod-like surface. The activity of Cu: ZnO/ TiO_2 photocatalyst was influenced by such dopant content and calcination temperature.

CONFLICT OF INTEREST

The authors declare that there are no conflicts of interest regarding the publication of this manuscript.

REFERENCES

1. Cermenati L, Dondi D, Fagnoni M, Albin A. Titanium

- dioxide photocatalysis of adamantane. *Tetrahedron*. 2003;59(34):6409-6414.
2. Li P, Li J, Wu C, Wu Q, Li J. Synergistic antibacterial effects of β -lactam antibiotic combined with silver nanoparticles. *Nanotechnology*. 2005;16(9):1912-1917.
3. Gamage J, Zhang Z. Applications of Photocatalytic Disinfection. *International Journal of Photoenergy*. 2010;2010:1-11.
4. Zhu J, Deng Z, Chen F, Zhang J, Chen H, Anpo M, et al. Hydrothermal doping method for preparation of Cr^{3+} - TiO_2 photocatalysts with concentration gradient distribution of Cr^{3+} . *Appl Catal B Environ*. 2006;62(3-4):329-335.
5. Schneider J, Matsuoka M, Takeuchi M, Zhang J, Horiuchi Y, Anpo M, et al. Understanding TiO_2 Photocatalysis: Mechanisms and Materials. *Chem Rev*. 2014;114(19):9919-9986.
6. Yusoff R, Shamiri A, Aroua MK, Ahmady A, Shafeeyan MS, Lee WS, et al. Physical properties of aqueous mixtures of N-methyldiethanolamine (MDEA) and ionic liquids. *J Ind Eng Chem*. 2014;20(5):3349-3355.
7. Sunada K, Kikuchi Y, Hashimoto K, Fujishima A. Bactericidal and Detoxification Effects of TiO_2 Thin Film Photocatalysts. *Photocatal Environ Sci Technol*. 1998;32(5):726-728.
8. Lowy FD. Staphylococcus aureus Infections. *N Engl J Med*. 1998;339(8):520-532.
9. Safardoust-Hojaghan H, Amiri O, Salavati-Niasari M, Hassanpour M, Khojasteh H, Foong LK. Performance improvement of dye sensitized solar cells based on cadmium sulfide/S, N co doped carbon dots nanocomposites. *Journal of Molecular Liquids*. 2020;301:112413.
10. Esmaili-Bafghi-Karimabad A, Ghanbari D, Salavati-Niasari M, Safardoust-Hojaghan H. Microwave-assisted synthesis of SiO_2 nanoparticles and its application on the flame retardancy of poly styrene and poly carbonate nanocomposites. *Journal of Nanostructures*. 2015;5(3):263-269.